

# Ab-initio optical spectra of complex systems

E. Cannuccia, O. Pulci, M. Palumbo, V. Garbuio, and R. Del Sole\*

ETSF and Dipartimento di Fisica dell'Università di Roma Tor Vergata, via della Ricerca Scientifica, 00133 Roma, Italy

Received 10 September 2007, revised 31 January 2008, accepted 2 February 2008

Published online 26 May 2008

PACS 31.15.E-, 71.35.Cc, 78.20.Bh

\* Corresponding author: e-mail [rodolfo.delsole@roma2.infn.it](mailto:rodolfo.delsole@roma2.infn.it), Phone: +39-06-72594597, Fax: +39-06-2023507

We review the theoretical framework of *ab-initio* excited state properties calculations showing the application of these methods to systems of different dimensionality. Many body perturbation theory within the GW approximation of the self energy for the calculation of electronic band structures is presented and applied to liquid water.

The Bethe Salpeter equation for the computation of optical properties is illustrated and used for the case of surfaces and liquid water. An alternative method for the calculation of optical properties, the Time Dependent Density Functional Theory, is also briefly illustrated.

© 2008 WILEY-VCH Verlag GmbH & Co. KGaA, Weinheim

**1 Introduction** Many experimental techniques in solid state physics, such as angle resolved photoemission spectroscopy (ARPES), electron energy loss (EELS), optical absorption etc... probe the electronic excitations of the systems under investigation. As a consequence, a material is often characterised by its excited state properties. A completely *ab-initio*, parameter free, determination of the excited state properties of materials is thus very important for the interpretation of the experimental spectra and/or for the prediction of the material's features. In this paper we will review the well established theoretical background of the *state of the art* calculation of excited state properties and we will show how these methods can be applied to systems of different dimensionality.

Almost all the calculations presented in this paper are performed using codes [1] that employ plane wave basis set. This kind of basis set allows for the intensive use of fast algorithms such as fast Fourier transforms (FFT) and moreover allows a systematic check on the convergence of the calculation. Plane waves are suited to describe crystal bulk systems in which a certain unit cell is repeated in all the three directions in space. However as we will show below, also lower dimensionality systems such as surfaces, molecules and disordered systems such as liquid water can be studied within the same scheme. Of course in all these

cases special care has to be put in order to avoid spurious effects due to the infinite reproduction of the unit cell, the so called *supercell*. For 0D systems, as molecules, the use of real space methods instead of plane waves is computationally more efficient. We will come back to this point in Section 5.

The paper is organized as follows. Section 2 is devoted to a brief review of the theory: first, ground state calculations within density functional theory (DFT), preliminary to all the excited state calculations, will be presented.

Then, we will see how quasiparticle effects can be introduced to get a reliable description of the electronic band structure. Finally we will see how many body effects, such as the excitonic effects, can be introduced in the calculations of optical spectra. We will show the results of calculations for surfaces (Section 3) and liquid water (Section 4). Finally, an alternative method for the calculation of optical properties, Time Dependent Density Functional Theory (TDDFT) will be shortly discussed and its application to a molecule of biological interest, the flavin, will be shown in Section 5. Conclusions are drawn in Section 6.

**2 Theoretical background** In this section we will briefly discuss the main equations of the theoretical *ab-initio* framework used here, in order to resume the different levels of approximations.

First, through a DFT [4, 5] calculation within Local Density Approximation (LDA) [6], with the use of norm-conserving pseudopotentials [7], the geometrical structure of the relaxed ground state configuration of the system has been obtained, solving self-consistently the one-particle Kohn-Sham (KS) equations [8]:

$$\left[-\frac{1}{2}\nabla^2 + V_{ext}(\mathbf{r}) + V_H(\mathbf{r}) + V_{xc}(\mathbf{r})\right] \cdot \varphi_i(\mathbf{r}) = \epsilon_i \varphi_i(\mathbf{r}) \quad (1)$$

where  $V_{ext}$  is the external potential due the ions,  $V_H$  is the Hartree potential,  $V_{xc}$  is the exchange-correlation potential of *DFT*.

Being the DFT a ground state theory, there is no rigorous justification to interpret the KS eigenvalues  $\epsilon_i$  as electron addition or removal energies. As a consequence, the calculated DFT-LDA electronic band gaps of semiconductors and insulators severely underestimate the experimental ones [9, 10]. Moreover it is well known [10] that also the optical spectra calculated at the DFT-LDA level, not only underestimate peak energies, but miss relative peak intensities. In order to give a proper description of the electronic excited states of a system, the Green's function formalism can be used [10]. The quasi-particle excitation energies are the poles of the one-particle Green function and are determined as solutions of the quasi-particle equation which is similar to the Kohn-Sham equation, where a non hermitian, non-local, energy dependent self-energy operator  $\Sigma$  [11, 12] replaces the exchange-correlation potential. In practical calculations the self-energy is approximated by the product of the Kohn-Sham Green function  $G$  times the screened Coulomb interaction  $W$  obtained within the Random Phase Approximation (RPA):  $\Sigma = iGW$  (see Ref. [9] and references therein). Moreover, a first-order perturbative solution of quasi-particle equation is used, with respect to  $\Sigma - V_{xc}$ . In this way the quasi-particle energies are obtained as:

$$\epsilon_i^{QP} = \epsilon_i^{LDA} + \frac{1}{1 + \beta_i} \langle \varphi_i^{LDA} | \Sigma(\epsilon_i^{LDA}) - V_{xc}^{LDA} | \varphi_i^{LDA} \rangle \quad (2)$$

where the superscript LDA indicates that KS eigenvalues and eigenvectors are calculated within the LDA;  $\beta_i$  is the linear coefficient in the energy expansion of  $\Sigma$  and  $i$  stays for the band index ( $v$  or  $c$ ) and for the wave vector  $\mathbf{k}$ .

Once the quasi-particle energies and wavefunctions are known we are able to evaluate the macroscopic dielectric function  $\epsilon_M(\omega)$  which can be compared to the experimental data. Indeed  $\epsilon_M(\omega)$  is defined as [13, 14]:

$$\epsilon_M(\omega) = \lim_{\mathbf{q} \rightarrow 0} \frac{1}{\epsilon_{\mathbf{G}=0, \mathbf{G}'=0}^{-1}(\mathbf{q}, \omega)} \quad (3)$$

This formula relies on the fact that, although in an inhomogeneous material the macroscopic field varies with frequency  $\omega$  and has a Fourier component of vanishing wavevector, the microscopic field varies with the same frequency but with different wavevectors  $\mathbf{q} + \mathbf{G}$ . These microscopic fluctuations induced by the external perturbation are at the origin of the local-field effects (LF) and reflect the spatial anisotropy of the material. The evaluation of  $\epsilon_M(\omega)$  within the linear response theory, in the independent particle approximation leads to the RPA dielectric function.

At this level, even if GW corrections are included, still no good agreement with the experimental results is guaranteed. In particular one may find optical spectra with peaks often at higher energies than the experimental ones and with wrong relative intensities.

In order to describe correctly the spectroscopic processes, where electron-hole pairs are created, the inclusion of the self-energy corrections alone, to the DFT eigenvalues, and the inclusion of local-field effects, are still not enough. The solution of the Bethe-Salpeter equation (BSE), where the coupled electron-hole excitations are included [10], is often required. Detailed discussions about this equation are already present in the literature [10, 15]; here, we just recall that its solution involves the study of the following excitonic hamiltonian :

$$H_{exc}^{(n_1, n_2), (n_3, n_4)} = (E_{n_2} - E_{n_1}) \delta_{n_1, n_3} \delta_{n_2, n_4} - i(f_{n_2} - f_{n_1}) \times \int d\mathbf{r}_1 d\mathbf{r}'_1 d\mathbf{r}_2 d\mathbf{r}'_2$$

$$\phi_{n_1}(\mathbf{r}_1) \phi_{n_2}^*(\mathbf{r}'_1) \Xi(\mathbf{r}_1, \mathbf{r}'_1, \mathbf{r}_2, \mathbf{r}'_2) \phi_{n_3}^*(\mathbf{r}_2) \phi_{n_4}(\mathbf{r}'_2)$$

where  $n_i$  refer to energy indexes of Kohn-Sham states. The kernel  $\Xi$  contains two contributions:  $\bar{v}$ , which is the bare coulomb interaction where the long range part corresponding to vanishing wave vector is not included (which describes local-field effects), and  $-W$ , the attractive screened coulomb electron-hole interaction. Using this formalism and considering only the resonant part of the excitonic hamiltonian [10], the macroscopic dielectric function comes out to be:

$$\epsilon_M(\omega) = 1 + \lim_{\mathbf{q} \rightarrow 0} v(\mathbf{q}) \times \sum_{\lambda} \frac{|\sum_{v,c;\mathbf{k}} \langle v, \mathbf{k} - \mathbf{q} | e^{-i\mathbf{q}\mathbf{r}} | c, \mathbf{k} \rangle A_{\lambda}^{(v,c;\mathbf{k})}|^2}{(E_{\lambda} - \omega)} \quad (4)$$

In Eq. (4) the dielectric function, differently from the RPA approximation, is given by a mixing of single particle transitions weighted by the excitonic eigenvectors  $A_{\lambda}$ . Moreover the excitation energies in the denominator are changed from  $\epsilon_c - \epsilon_v$  (single particle energy transitions) to  $E_{\lambda}$  which are the excitonic eigenvalues.

### 3 Application to surfaces

**3.1 The case of GaP(110)** Great amount of theoretical and experimental data has been published on the technologically important GaAs and GaN surfaces, but also the other III-V compounds (InAs, InP, GaP and so on) have been the subject of many fundamental studies. The (110), being the cleavage plane of III-V compounds, is the most natural choice for basic studies, since it is easily prepared with a well defined stoichiometry, a feature nearly all other III-V surfaces do not have. The (110) surface is relaxed but not reconstructed [16–18], with the anion atom moving outwards the surface plane, and the cation inwards. Also the electronic band structure of the III-V(110) are remarkably similar, all with a fundamental gap free of surface states and two surface bands,  $C_3$  and  $A_5$ , arising from cation and anion dangling bonds, clearly detected by direct and inverse photoemission [19]. The only exception to this general trend seemed to be represented, for some time, by the GaP(110) surface, that was believed to have surface states within the fundamental gap. Another characteristic that differentiates GaP from most of the other III-V compounds is its fundamental indirect gap ( $\Gamma - X \sim 2.35$  eV [20], to be compared with a theoretical value, obtained at a DFT level, of 1.5 eV, and a GW gap of 2.3 eV).

Although many experimental results have been published on GaP(110) (see for example [19], [21], [22] and references therein), its optical properties have been studied, so far, only within the Tight Binding [22] and DFT [23] methods. Here, in order to illustrate the importance of the inclusion of Many-Body effects, we show calculations of its optical properties, namely its Reflectance Anisotropy Spectrum (RAS), with the inclusion of GW corrections. RAS is defined as:

$$\frac{\Delta R}{R} = 2 \frac{R_y - R_x}{R_y + R_x} \quad (5)$$

where  $R_x$  and  $R_y$  are the reflectivity along  $x$  and  $y$  in-plane directions. For GaP(110), we select  $x$  along the [001] and  $y$  along the  $[\bar{1}10]$  directions.

Our calculated RAS, at the DFT and GW level, is shown in Fig. 1 together with experimental results by [22]. A trend common to all the (110) surfaces is clearly visible: a) the reflectance for light polarized along the surface atomic chains ( $[\bar{1}10]$  direction) dominates over that along the [001] direction (perpendicular to the atomic chains); b) optical structures appear in the vicinity of bulk critical points.

The experimental peak at 2.7 eV originates, in our GW calculation, from surface states transitions at  $\bar{X}$ . All the other structures are bulk-related, with the experimental dip around 3.7 eV followed by the peak at 3.9 eV probably related to transitions near  $E_1$  (GW gap at L: 3.9 eV; DFT gap at L: 3.0 eV). Finally, the strong absorption structure at 5.2 eV corresponds to the position of the  $E_2$  bulk transition (GW gap at X: 5.1 eV; DFT gap at X: 4.3 eV).

Although the agreement between theory and experiment is far from being perfect, we can safely affirm that

### GaP(110)

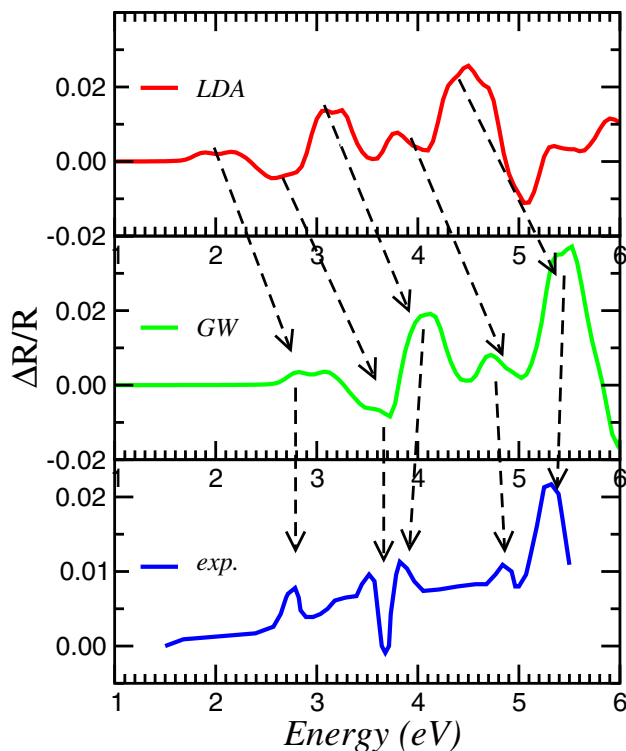


**Figure 1** Reflectance anisotropy spectrum of the GaP(110) surface at the DFT and GW level. Also experimental results by [22] are shown.

the main characteristic of the measured RAS are well represented in the GW calculations. Instead the DFT spectrum, because of the DFT underestimation of the electronic gaps, is unable to correctly describe the experimental RAS. Moreover, it is clear that excitonic effects, not included here, may have some effects on the intensity of the surface related peak at 2.7 eV.

**3.2 Electron energy loss of C(100)** The C(001) surface reconstructs in a  $2 \times 1$  dimerized geometry. At odd with the Si(001) $2 \times 1$ , the C-C dimers are not buckled, and their bond length is about 1.37 Å [24], [25], [26], [27], [28], [29]. C(001) $2 \times 1$  represents a case where excitonic effects play a fundamental role in the RAS [29], [30]. This is due to the fact that surface bands are well separated from bulk bands, so that exciton dynamics is effectively two dimensional and to the reduced screening at the surface with respect to bulk.

The importance of excitonic effects in this surface is also clearly visible in the EELS spectrum [24]: in Fig. 2 the theoretical EEL spectra, obtained including Many-Body effects (panel b) are compared with the experiments of ref. [31] (panel a). The experiment was performed with a primary beam energy of 50 eV and at a fixed angle of in-

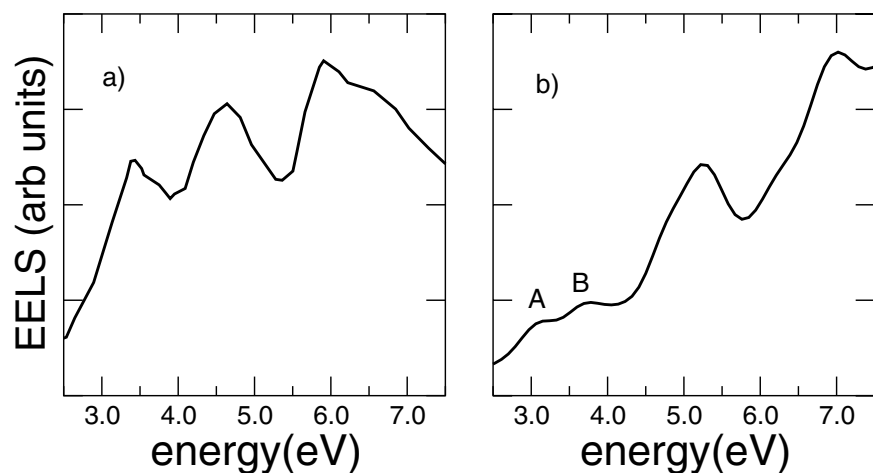


**Figure 2** Electron energy loss spectrum of C(100)  $2 \times 1$  surface. (a) Experimental spectrum from ref. [31]. (b) Theoretical spectrum with excitonic effects included. A and B refer to two surface-state excitons (see the text and Ref. [24] for more details.)

idence  $\phi_i = 60^\circ$  under specular reflection. Thanks to the high energetic primary beam and to the small energy loss, the use of dipole-scattering theory is allowed and the comparison of theoretical results with the experimental curve is justified. A typical value of the transferred momentum in this experimental configuration is  $q_{\parallel} \simeq 0.15$  a.u.

The experimental loss function is characterized by three main peaks located at 3.5, 4.7 and 5.9 eV. We can see that the agreement of the theoretical results with the experiment is reasonably good (panel b). The lowest energy double-peak (centered around 3.5 eV) is due to the excitation of the surface-state excitons, appearing at 3.1 and 3.8 eV (A and B in the right panel of Fig. 2) in the surface dielectric functions; the calculated double peak corresponds well to the asymmetric experimental structure around 3.4 eV. The calculated structure at about 5 eV is due to surface state-surface state transitions, and the higher structures are mixed surface state-bulk state transitions.

#### 4 Disordered systems: the example of liquid water

As an example of GW and BSE calculation in complex systems, we show the results obtained within this theory for a particular three dimensional system: liquid water [32]. The peculiar problem related to the study of a liquid disordered system relies on the fact that one should in principle use a very large unit cell. A possible solution to avoid such huge unit cells has been proven [32] to be the use of smaller unit cells but exploiting several molecular dynamics (MD) snapshots of water as input geometries and averaging the results over all the configurations. We used 20 configurations of 17 water molecules in a cubic box with 15 a.u. side. We firstly used DFT to obtain Kohn-Sham eigenvalues and eigenvectors and then corrected the energy levels within the GW approximation. In the calculations we used GGA pseudopotentials and 8 k-points to sample the Brillouin zone. [33]

DFT-KS results for the electronic properties of water (obtained averaging over the 8 k points for each of the 20 configurations) are shown in Fig. 3. The configuration-

averaged HOMO-LUMO gap turned out to be 5.09 eV, in good agreement with previous DFT calculations [34] but strongly underestimating the experimental gap ( $8.7 \pm 0.5$  eV [35]), as expected in DFT.

In order to correct the KS electronic gap we calculated the GW corrections  $\Delta\varepsilon_n^{QP}$  to the KS energies. This should be done for *all* the 20 MD configurations, followed by an average. In particular the calculation of the screened Coulomb interaction for 20 configurations constitutes a true bottleneck. Instead, we observed that the GW corrections  $\Delta\varepsilon_n^{QP}$  were quite stable with respect to the configuration. In other words, the difference between DFT and GW,

$\Delta GW = \varepsilon_n^{QP} - \varepsilon_n^{DFT}$ , was practically constant going from one snapshot to another. This is explicitly shown in Table 1 for three different configurations. We used, hence, the same GW corrections for all the DFT configurations. With this GW corrections the average electronic HOMO-LUMO gap is increased to 8.4 eV well within the experimental range ( $8.5 \pm 0.5$  eV) [35], as shown in Fig. 3. Nevertheless, the optical spectrum obtained within GW is completely at odd with experiment. Our GW results, averaged over the 20 MD configurations are shown in Fig. 4: both the peak positions and relative intensities are wrong, suggesting dramatic many-body effects in liquid water. In fact, agreement with experiment both in energy peak positions and onset, as well as in the relative intensities of the first two peaks, is significantly improved when using the BSE approach.

**Table 1** GW corrections to the HOMO and LUMO energy levels and to the GGA electronic gap, for three different water configurations (E19, E8, E2). Energies in eV.

	DFTgap	$\Delta GW$ HOMO	$\Delta GW$ LUMO	$\Delta GW$ gap
E19	5.09	-1.67	1.61	3.28
E8	4.71	-1.64	1.60	3.24
E2	5.29	-1.70	1.60	3.30

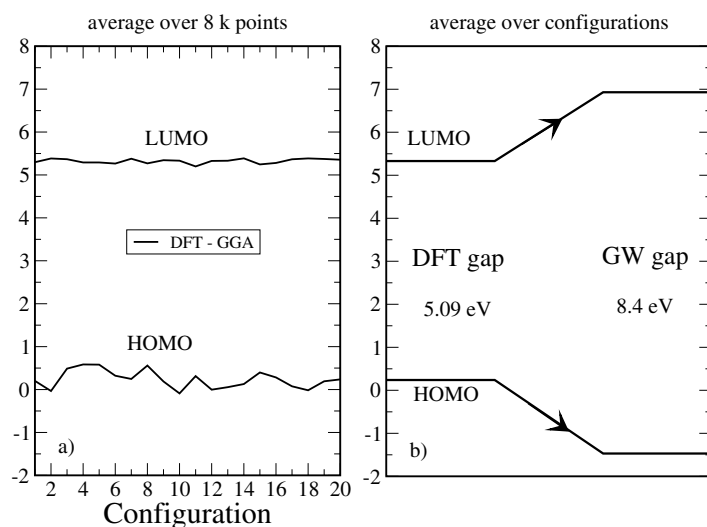


**Figure 3** a) DFT HOMO and LUMO energies, averaged over the 8 k-points, for the 20 MD configurations of liquid water. b) Schematic DFT and GW HOMO-LUMO gaps, averaged over the 20 MD configurations.

We show in Fig. 4 the excitonic spectra for all the 20 MD configurations (yellow lines) and their average (red line). The main remaining discrepancy between theory and experiment is an overall redshift, that might be due to the fact that our GW calculations are not self-consistent but use DFT wavefunctions and energies. The first peak in the spectrum turns out to be a bound exciton with a binding energy of 2.4 eV and large oscillator strength. These are a consequence of the weak electronic dielectric screening of water ( $\epsilon_\infty \sim 1.8$ ). The second peak results from an excitonic enhancement of the oscillator strength of interband transitions with respect to the single quasi-particle case.

**5 The time dependent density functional approach** In the previous section we have seen that an accurate description of optical spectra can be obtained within the Bethe Salpeter approach. In order to solve the excitonic hamiltonian, first of all one has to perform a well converged DFT calculation, as a second step GW corrections to the DFT eigenvalues have to be calculated, and as a third step the Bethe Salpeter equation is finally solved. The 3 steps here described are of increasing difficulty. It is hence clear that this approach can not be applied to very complex systems, and as a matter of fact full GW and Bethe Salpeter calculations have been done on systems composed of a maximum few tens of atoms.

On the other hand, DFT can be applied easily to very large systems (hundreds of atoms). Density Functional Theory, described in Section 2, is a ground state theory in which the charge density is the relevant physical quantity. DFT has proven to be very successful in describing structural and electronic properties for a vast class of materials and furthermore is computationally not demanding. For these reasons DFT has become a common tool in first principles calculations for the description of molecular and

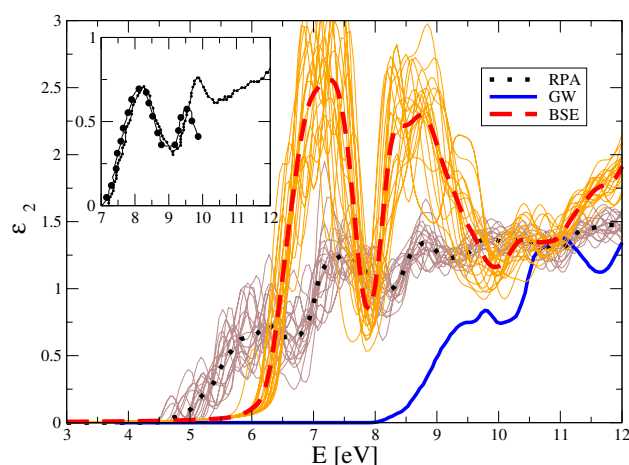


**Figure 4** Optical absorption spectrum of liquid water averaged over the different MD configurations, calculated at different theoretical levels: DFT-RPA (black dots), GW (blue) and with the inclusion of excitonic effects (BSE, red curve). In yellow we show also the BSE results for all different configurations which, averaged, give the red curve. Inset: experimental data from [36, 37].

condensed matter systems properties. Anyway, as already mentioned, DFT cannot reproduce some quantities such as electronic excitations energies and optical spectra, being a ground state theory. A rigorous generalization of DFT to time dependent external fields was proposed by Runge, Gross and Kohn [38, 39]. In the work of Runge and Gross a theory similar to the Hohenberg-Kohn-Sham has been developed, but for time-dependent potentials. Several reviews of the foundation of TDDFT and its applications can be found [40–42]. In contrast to DFT, no energy minimum

principle is available and the evolution of the system is described by the quantum-mechanical action, defined by Eq. (6). The true time dependent density is the one which makes the action stationary.

$$A[\Psi] = \int_{t_0}^{t_1} dt \langle \Psi(t) | i \frac{\partial}{\partial t} - H(t) | \Psi(t) \rangle. \quad (6)$$

where  $H(t)$  and  $\Psi(t)$  are the t-dependent hamiltonian and eigenfunction of the system,  $t_0$  is the initial time, when the time-dependent perturbation starts to be applied, and  $t_1$  is a generic final time. Minimizing the action it is possible to obtain a set of time dependent KS equations, given by:

$$\left[ -\frac{1}{2} \nabla^2 + v_{eff}(\mathbf{r}, t) \right] \phi_i(\mathbf{r}, t) = i \frac{\partial}{\partial t} \phi_i(\mathbf{r}, t) \quad (7)$$

where we assume the existence of a potential  $v_{eff}(\mathbf{r}, t)$

$$v_{eff}(\mathbf{r}, t) = v_{ext}(\mathbf{r}, t) + \int \frac{n(\mathbf{r}, t)}{|\mathbf{r} - \mathbf{r}'|} d\mathbf{r}' + V_{xc}(\mathbf{r}, t) \quad (8)$$

for an independent particle system whose orbitals  $\phi_i(\mathbf{r}, t)$  yield the same charge density  $n(\mathbf{r}, t)$  of the interacting system,

$$n(\mathbf{r}, t) = \sum_{i=1} f_i |\phi_i(\mathbf{r}, t)|^2. \quad (9)$$

Since all observables are unique functionals of the density, in principle any property can be exactly obtained by the Kohn-Sham time-dependent formalism. The simplest possible approximation of the time-dependent xc potential is the so called adiabatic local density approximation (ALDA). It employs the functional form of the static LDA with a time-dependent density:

$$V_{xc}^{ALDA}[n](\mathbf{r}, t) = V_{xc}^{LDA}(n(\mathbf{r}, t)) = \frac{d}{dn} (n \epsilon_{xc}^{hom}(n)) |_{n=n(\mathbf{r}, t)} \quad (10)$$

If we are interested in optical spectra, we can use a method based on the time evolution of the Kohn and Sham equations [43], [44]. Let be  $\phi_i(\mathbf{r})$  the KS wave functions of ground state, with which the initial state of the system is built. The system is excited by an electric field:

$$\delta v_{est}(\mathbf{r}, t) = -k_0 r_\nu \delta(t), \quad (11)$$

where  $\nu = x, y, z$ . In order to consider the response of the system as linear, the amplitude  $k_0$  must be small. At  $t = 0^+$  the initial state for the time evolution is given by:

$$\begin{aligned} \phi_i(\mathbf{r}, t = 0^+) &= \\ \hat{T} \exp \left\{ -i \int_0^{0^+} dt \left[ \hat{H}_{KS} - k_0 r_\nu \delta(t) \right] \right\} \phi_i(\mathbf{r}) \\ &= \exp(ik_0 r_\nu) \phi_i(\mathbf{r}). \end{aligned} \quad (12)$$

where  $H_{KS}$  is the ground-state KS hamiltonian. The induced charge is

$$\delta n(\mathbf{r}, \omega) = \int d\mathbf{r}' \chi(\mathbf{r}, \mathbf{r}', \omega) \delta v_{est}(\mathbf{r}', \omega), \quad (13)$$

where  $\chi$  is the response function of the interacting system. The dynamical polarizability can be obtained from

$$\alpha_\nu(\omega) = -\frac{1}{k_0} \int d\mathbf{r} r_\nu \delta n(\mathbf{r}, \omega), \quad (14)$$

which in the dipole approximation becomes

$$\alpha_\nu(\omega) = - \int d\mathbf{r} \int d\mathbf{r}' r_\nu \chi(\mathbf{r}, \mathbf{r}', \omega) r'_\nu. \quad (15)$$

In the expression (13),  $\delta n(\mathbf{r}, \omega)$  is the Fourier transform of  $n(\mathbf{r}, t) - \tilde{n}(\mathbf{r})$ , where  $\tilde{n}(\mathbf{r})$  is the ground state density of the system. The quantity obtained in an experiment of photoabsorption, is the cross section, given by:

$$\sigma(\omega) = \frac{4\pi\omega}{c} \frac{1}{3} \Im \sum_\nu \alpha_\nu(\omega), \quad (16)$$

where  $c$  is the speed of light.

This method, in the ALDA approximation for  $v_{xc}$ , is often used with success to calculate the absorption spectra of finite systems, from small molecules to biological systems.

We applied the Time Dependent Density Functional Theory (TDDFT) to the flavin mononucleotide (FMN) in its oxidized form. We used the LDA approximation (for the correlation part we used the Perdew and Wang parametrization [45]) and Troullier-Martins pseudopotentials [7].

In order to calculate the optical spectrum, we replaced the "chain" of flavine mononucleotide [46] with a methyl group  $CH_3$ , because only the chromophore (the system with the three rings) is optically reactive. This molecule is called lumi-flavine and is shown in Fig. 5.

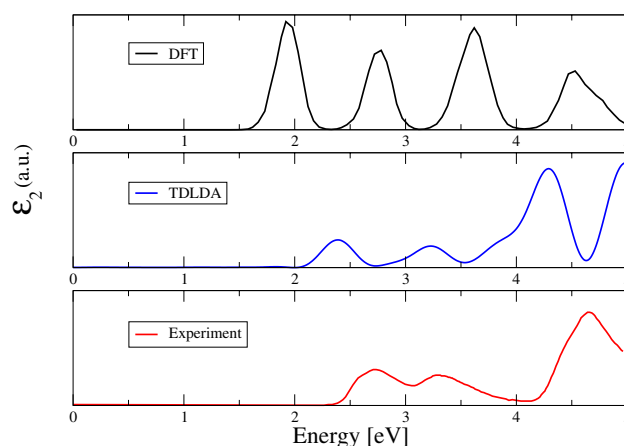
The numerical calculations have been performed with the Octopus code [47], which solves the Kohn-Sham equations on a grid in real space using null boundary conditions. For this reason Octopus is a suitable code especially for finite systems like the molecules. Real space

**Figure 5** Oxidized lumiflavin.

methods are of course better suited for finite systems so that no artificial periodicity has to be introduced.

The wave functions are represented by their value over a set of points in real space. The separation between points, or spacing, is a critical parameter. This parameter is equivalent to the energy cutoff used by plane waves representations. The shape of the simulation region may also be tuned to suit the geometric configuration of the system: we chose a sphere built around each atom. After some convergence tests, we have fixed the spacing on 0.18 Å, (which corresponds to a cut-off kinetic energy of 85 Ry) and the radius of the spheres of 5 Å. With these parameters we calculated the optical spectrum, evolving the wave functions for a period of  $4 \times 10^{-16}$  s.

In Fig. 6 we show our results for the lumiflavin in the oxidized form: the spectrum is calculated at the DFT (RPA, non local fields) level, and at the TDDFT level. The DFT spectrum has been calculated using Espresso PWSCF [48] code with a kinetic cutoff energy of 60 Ry, with an orthorhombic cell of sides  $a = 30$  a.u.,  $b = 26.8$  a.u. and  $c = 21.4$  a.u. respectively along x, y, z directions (see Fig. 5) and with BLYP pseudopotentials [49]. The TDDFT spectrum has been calculated with a spacing of 0.18 Å and radius of the spheres of 5 Å. The experimental spectrum, instead, also shown in Fig. 6, refers to flavin mononucleotide in solution. (To our knowledge, there are no published experimental gas-phase spectra of FMN because of the low volatility of flavins, hence we refer to the experimental spectrum of FMN in aqueous solution [50], [51]). Whereas the DFT spectrum is unable to reproduce the position and the relative intensities of the experimental absorption peaks, the agreement of the TDLDA spectrum with the experimental one is very good. A small (about 0.37 eV) shift between theory and experiment can be observed, maybe to the fact that the experimental spectrum refers to flavin in water and not in vacuum.

**Figure 6** Optical spectra of the oxidized lumiflavin obtained at different level of the theoretical approximation (top and central panels) compared with the experimental data (bottom panel) from Ref. [51]

**6 Conclusion** We have shown that parameter-free calculations of the spectroscopic properties of systems with different dimensionality and microscopic order, are now possible using Many-Body Perturbation Theory to correct the failures of the one-particle DFT approach. This scheme allows to determine both ground state and excited state properties at the same level of microscopic accuracy. We have discussed self-energy effects in the GW approximation which yields quite accurate results for the electronic gaps in many materials. Moreover, we have introduced the Bethe-Salpeter equation needed to describe the electron-hole interaction and shown some examples where theoretical response are strongly influenced by many body effects. An alternative approach, TDDFT, which is computationally quicker than the BSE, has also been discussed. As an example, its application to a molecule of biological interest, the flavin, has been illustrated.

**Acknowledgements** This work has been supported by MIUR project PRIN NANOEXC 2005, MIUR project NANOSIM, by the EU through the Nanoquanta Network of Excellence (NMP4-CT-2004-500198) and by CNISM. Computer resources from INFN “Progetto Calcolo Parallelo” at CINECA are gratefully acknowledged.

## References

- [1] The DFT-GGA calculations have been performed using the FHI98MD code [2], the PWSCF code: S. Baroni, S. de Gironcoli, A. Dal Corso, and P. Giannozzi, <http://www.pwscf.org/>, and the ABINIT code [3]. GW and

- BSE calculation have been performed using codes developed in the NANOQUANTA NoE <http://www.nanoquanta.eu>.
- [2] M. Bockstedte, A. Kley, J. Neugebauer, and M. Scheffler, *Comput. Phys. Commun.* **107**, 187 (1997).
- [3] X. Gonze, J.-M. Beuken, R. Caracas, F. Detraux, M. Fuchs, G.-M. Rignanese, L. Sindic, M. Verstraete, G. Zerah, F. Jollet, M. Torrent, A. Roy, M. Mikami, Ph. Ghosez, J.-Y. Raty, and D.C. Allan, *Comput. Mater. Sci.* **25**, 478 (2002).
- [4] P. Hohenberg and W. Kohn, *Phys. Rev. B* **136**, 864 (1964).
- [5] R. M. Dreizler and E. K. U. Gross *Density Functional Theory* (Springer-Verlag Heidelberg, 1990). R. O. Jones and O. Gunnarsson *Rev. Mod. Phys.* **61**, 689 (1989).
- [6] D. M. Ceperley and B. J. Alder, *Phys. Rev. Lett.* **45**, 566 (1980).
- [7] N. Troullier and J. L. Martins, *Phys. Rev. B* **43**, 19993 (1991).
- [8] W. Kohn and L. J. Sham, *Phys. Rev.* **140**, A1113 (1965).
- [9] F. Aryasetiawan and O. Gunnarsson, *Rep. Prog. Phys.* **61**, 237 (1998), and references therein.
- [10] G. Onida, L. Reining, and A. Rubio, *Rev. Mod. Phys.* **74**, 601 (2002), and references therein.
- [11] L. Hedin, *Phys. Rev.* **139**, A796 (1965).
- [12] L. Hedin and S. Lundqvist, in: *Solid State Physics*, edited by H. Ehrenreich, F. Seitz, and D. Turnbull (Academic Press, New York).
- [13] S. L. Adler, *Phys. Rev.* **126**, 413 (1962).
- [14] N. Wiser, *Phys. Rev.* **129**, 62 (1962).
- [15] M. Rohlfing and S. Louie, *Phys. Rev. B* **62**, 4927 (2000).
- [16] C. B. Duke, A. Paton, A. Kahn, and C. R. Bonapace, *Phys. Rev. B* **27**, 6189 (1983).
- [17] See for example, F. Bechstedt and R. Enderlein, *Semiconductor Surfaces and Interfaces* (Akademie-Verlag, Berlin, 1988); A. Zangwill, *Physics at Surfaces* (Cambridge University Press, New York, 1992); H. Lüth, *Surfaces and Interfaces of Solids* (Springer Verlag, Berlin, 1993).
- [18] T. J. Godin, J. P. LaFemina, and C. B. Duke, *J. Vacuum Sci. Technol. A* **10**, 2059 (1992).
- [19] H. Carstensen et al., *Phys. Rev. B* **41**, 9880 (1990).
- [20] O. Madelung (Ed.), *Landolt-Börnstein, Numerical Data and Functional Relationships in Science and Technology*, New Series, Vol. 17a (Springer-Verlag Berlin, 1982).
- [21] J. Van Laar et al., *J. Vacuum Sci. Technol.* **14**, 894 (1977).
- [22] A. Shkrebtii, N. Esser, M. Köpp, P. Haier, W. Richter, and R. Del Sole, *Appl. Surf. Sci.* **104/105**, 176 (1996).
- [23] F. Manghi, R. Del Sole, A. Selloni, and E. Molinari, *Phys. Rev. B* **41**, 9935 (1990).
- [24] M. Palumbo, O. Pulci, A. Marini, and L. Reining, *R. Del Sole, Phys. Rev. B* **74**, 1 (2006).
- [25] F. Maier, J. Ristein, and L. Ley, *Phys. Rev. B* **64**, 165411-1 (2001).
- [26] M. D. Winn, M. Rässinger, and J. Hafner, *Phys. Rev. B* **55**, 5364 (1997); Z. Zhang, M. Wensell, and J. Bernholc, *Phys. Rev. B* **51**, 5291 (1995).
- [27] J. Ristein, *Appl. Phys. A* **82**, 377-384 (2006). S. J. Sque, R. Jones, and P. R. Briddon, *Phys. Rev. B* **73**, 085313 (2006).
- [28] P. Kruger and J. Pollman, *Phys. Rev. Lett.* **74**, 1155 (1995).
- [29] M. Palumbo, O. Pulci, R. Del Sole, A. Marini, M. Schwitters, S. R. Haines, K. H. Williams, D. S. Martin, P. Weightman, and J. E. Butler, *Phys. Rev. Lett.* **94**, 087404 (2005).
- [30] O. Pulci, M. Palumbo, M. Marsili, and R. Del Sole, *Adv. Solid State Phys.* **45**, 161-172 (2005).
- [31] T. W. Mercer and P. E. Pehrsson *Surf. Sci.* **399**, L327-L331 (1998).
- [32] V. Garbuio et al., *Phys. Rev. Lett* **97**, 137402 (2006).
- [33] The Generalized Gradient Approximation (GGA) takes approximately into account the non locality of the xc potential [5].
- [34] K. Laasonen et al., *J. Chem. Phys.* **99**, 9080 (1993).
- [35] See e.g. A. Bernas et al., *Chem. Phys.* **222**, 151 (1997), and references therein; <http://www.ensta.fr/muguet/papers/ECCC7/band.html> and references therein.
- [36] G. D. Kerr et al., *Phys. Rev. A* **5**, 2523 (1972).
- [37] L. R. Painter et al., *Phys. Rev. Lett.* **21**, 282 (1968).
- [38] E. Runge and E. K. U. Gross, *Phys. Rev. Lett.* **52**, 997 (1984).
- [39] E. K. U. Gross and W. Kohn, *Phys. Rev. Lett.* **55**, 2850 (1985).
- [40] E. K. U. Gross, F. J. Dobson, and M. Petersilka, *Density Functional Theory* (Springer, New York, 1996).
- [41] M. Casida, *Recent Developments and Applications of Modern Density Functional Theory*, edited by J. M. Seminario (Elsevier Science, Amsterdam, 1996).
- [42] J. Dobson, G. Vignale, and M. P. Das, *Electronic Density Functional Theory: Recent Progress and New Directions* (Plenum, New York, 1997).
- [43] M. A. L. Marques, *A Tutorial on Density Functional Theory* (2003), pp. 144-184.
- [44] M. A. L. Marques and E. K. U. Gross, *Ann. Rev. Phys. Chem.* **55**, 427 (2004).
- [45] J. P. Perdew and Y. Wang, *Phys. Rev. B* **45**, 13244 (1992).
- [46] S.-H. Song, B. Dick, and A. Penzkofer, *Chem. Phys.* **332**, 55 (2006).
- [47] M. A. L. Marques, A. Castro, G. F. Bertsch, and A. Rubio, *Comput. Phys. Commun.* **151**, 60 (2003); more information can be found on [www.tddft.org/programs/octopus](http://www.tddft.org/programs/octopus).
- [48] S. Baroni, A. Dal Corso, S. de Gironcoli, P. Giannozzi, C. Cavazzoni, G. Ballabio, S. Scandolo, G. Chiarotti, P. Focher, A. Pasquarello, K. Laasonen, A. Trave, R. Car, N. Marzari, and A. Kokalj, <http://www.pwscf.org/>
- [49] J. P. Perdew, K. Burke, and M. Ernzerhof, *Phys. Rev. Lett.* **77**, 3865 (1996).
- [50] K. H. Dudley, A. Ehrenberg, P. Hemmerich, and F. Muller, *Helv. Chim. Acta* **47**, 1354 (1964).
- [51] C. Neiss, P. Saalfrank, M. Parac, and S. Grimme, *J. Phys. Chem. A* **107**, 140 (2003).